2. Efstathiou SF, Pefanis AV, Tsioulos DI *et al*. Acute pyelonephritis in adults: prediction of mortality and failure of treatment. *Arch Int Med* 2003; 163: 1206–1212.
3. Scholes D, Hooton TM, Roberts PL *et al*. Risk factors associated with acute pyelonephritis in healthy women. *Ann Intern Med* 2005; 142: 20–27.
4. Kawashima A, Le Roy AJ. Radiologic evaluation of patients with renal infections. *Infect Dis Clin North Am* 2003; 17: 433–456.
5. Majd M, Nussbaum Blask AR, Markle BM *et al*. Acute pyelonephritis: comparison of diagnosis with 99mTc-DMSA, SPECT, spiral CT, MR imaging, and power Doppler US in an experimental pig model. *Radiology* 2001; 218: 101–108.
6. Levey AS, Greene T, Kusek JW *et al*. A simplified equation to predict glomerular filtration rate from serum creatinine. *J Am Soc Nephrol* 2000; 11: 155A.
7. Fraser IR, Birch D, Fairley KF *et al*. A prospective study of cortical scarring in acute febrile pyelonephritis in adults: clinical and bacteriological characteristics. *Clin Nephrol* 1995; 43: 159–164.
8. Warren JW, Abrutyn E, Hebel JR *et al*. Guidelines for antimicrobial treatment of uncomplicated acute bacterial cystitis and acute pyelonephritis in women. Infectious Diseases Society of America (IDSA). *Clin Infect Dis* 1999; 29: 745–758.
9. Siegel JF, Smith A, Moldwin R. Minimally invasive treatment of renal abscess. *J Urol* 1996; 155: 52–55.
10. Meyrier A, Calderwood SB, Baron EL. Renal and perirenal abscess. http://www.uptodate.com/contents/renal-and-perinephric-abscess (7 December 2011, date last accessed).
11. Meyrier A, Guibert J. Diagnosis and drug treatment of acute pyelonephritis. *Drugs* 1992; 44: 56–59.
12. Wallin L, Bajc M. Typical technetium dimercaptosuccinic acid distribution patterns in acute pyelonephritis. *Acta Paediatr* 1993; 82: 1061–1065.
13. Majd M, Rushton HD, Jantausch B *et al*. Relationship among vesicoureteral reflux, P-fimbriated Escherichia coli, and acute pyelonephritis in children with febrile urinary tract infection. *J Pediatr* 1991; 119: 578–585.
14. Gupta K, Hooton TM, Naber KG *et al*. International clinical practice guidelines for the treatment of acute uncomplicated cystitis and pyelonephritis in women: a 2010 update by the Infectious Diseases Society of America and the European Society for Microbiology and Infectious Diseases. *Clin Infect Dis* 2011; 52: e103–e120.
15. Pertel PE, Haverstock D. Risks factors for a poor outcome after therapy for acute pyelonephritis. *BJU Int* 2006; 98: 141–147.

Received for publication: 2.5.2011; Accepted in revised form: 30.12.2011

Nephrol Dial Transplant (2012) 27: 3493–3501
doi: 10.1093/ndt/gfr811
Advance Access publication 8 February 2012

Arteriolar vascular smooth muscle cell differentiation in benign nephrosclerosis

Clemens Luitpold Bockmeyer[1,*], David Sebastian Kern[1,*], Vinzent Forstmeier[1], Svjetlana Lovric[2], Friedrich Modde[1], Putri Andina Agustian[1], Sandra Steffens[3], Ingvild Birschmann[4], Jana Traeder[1], Maximilian Ernst Dämmrich[1], Anke Schwarz[2], Hans Heinrich Kreipe[1], Verena Bröcker[1] and Jan Ulrich Becker[1]

[1]Institute of Pathology, Hannover Medical School, Hannover, Germany, [2]Department of Nephrology and Hypertension, Hannover Medical School, Hannover, Germany, [3]Clinic for Urology, Hannover Medical School, Hannover, Germany and [4]Clinic for Haematology, Haemostaseology and Oncology, Hannover Medical School, Hannover, Germany

Correspondence and offprint requests to: Jan Ulrich Becker; E-mail: JanBecker@gmx.com
*Both authors contributed equally to this work.

Abstract

Background. Benign nephrosclerosis (bN) is the most prevalent form of hypertensive damage in kidney biopsies. It is defined by early hyalinosis and later fibrosis of renal arterioles. Despite its high prevalence, very little is known about the contribution of arteriolar vascular smooth muscle cells (VSMCs) to bN. We examined classical and novel candidate markers of the normal contractile and the pro-fibrotic secretory phenotype of VSMCs in arterioles in bN.

Methods. Sixty-three renal tissue specimens with bN and eight control specimens were examined by immunohistochemistry for the contractile markers caldesmon, alpha-smooth muscle actin (alpha-SMA), JunB, smoothelin and the secretory marker S100A4 and by double stains for caldesmon or smoothelin with S100A4.

Results. Smoothelin immunostaining showed an inverse correlation with hyalinosis and fibrosis scores, while S100A4 correlated with fibrosis scores only. Neither caldesmon, alpha-SMA nor JunB correlated with hyalinosis or fibrosis scores. Cells in the arteriolar wall were exclusively positive either for caldesmon/smoothelin or S100A4.

Conclusions. This is the first systematic analysis of VSMC differentiation in bN. The results suggest that smoothelin is the most sensitive marker for the contractile phenotype and that S100A4 could be a novel marker for the secretory

phenotype *in vivo*. The other markers did not seem to differentiate these phenotypes in bN. Thus, VSMC phenotype markers should be defined in the context of the vessel segment and disease under examination. S100A4 could not only be a marker of pro-fibrotic secretory VSMCs in bN but also an important mediator of arteriolar fibrosis.

Keywords: arteriolosclerosis; arterionephrosclerosis; hypertensive nephrosclerosis; vascular smooth muscle cell; FSP1

Introduction

Benign nephrosclerosis (bN), defined as kinking, hyalinosis and fibrosis of small preglomerular vessels [1], is a very common finding in renal biopsies. While considerable effort has been made to characterize the glomerular and tubulointerstitial manifestations of hypertensive renal damage; surprisingly, little is known about the changes in the affected vessels themselves.

The main constituent cell of the arterial and arteriolar wall is the vascular smooth muscle cell (VSMC). It is also functionally important for the autoregulation of glomerular blood flow and capillary pressure [2]. Smooth muscle cells have been the subject of extensive studies in diseases of the bronchi (reviewed in [3, 4]), pulmonary arteries (reviewed in [5–7]) and systemic arteries (reviewed in [8, 9]). Based on these studies and *in vitro* experiments, a paradigm of the contractile and the secretory phenotype has been developed [10, 11]. The normal physiological phenotype of VSMCs is called the contractile phenotype. The (collagen-) secretory phenotype is considered pathological. Although never formally proven in humans, the current concept of bN claims that the initial stage of bN is the hyalinotic lesion. This hyalinosis is thought to later transform into the fibrotic lesion [1]. Based on this assumption and on the paradigm above, we hypothesized that during the hyalinotic lesion, arteriolar VSMCs (aVSMCs) retain their contractile phenotype and that a transition towards the secretory phenotype is required for the transformation of the hyalinotic to the fibrotic lesion. We have recently shown that ADAMTS13 (a disintegrin and metalloproteinase with a thrombospondin type 1 motif, member 13), the von Willebrand factor cleaving protease, and smoothelin could serve as markers of the contractile phenotype [12].

Building on the foundation of our previous study which included only contractile markers, we tested this hypothesis in a larger cohort of human renal tissue. Furthermore, we examined a wider range of differentiation markers, including the candidate marker for the secretory phenotype S100A4, and we did double stains to explore the shift in differentiation of the aVSMCs.

Materials and methods

Tissue samples

Sixty-three renal tissue samples (55 biopsies and 8 nephrectomy specimens due to laceration or tumour) with an isolated diagnosis of bN were chosen from the archive of the Institute of Pathology, Hannover Medical School, Hannover, Germany. Excluded were tissue specimens with any other primary vascular, glomerular or tubulointerstitial disease.

All biopsies were subject to routine histological workup including multiple haematoxylin and eosin-, periodic acid-Schiff (PAS)- and Jones sections, immunohistochemistry for IgA, IgG, IgM, C1q and C3c and ultrastructural examination of at least one glomerulus.

These biopsies were compared to normal control kidney specimens from eight patients from tumour or trauma nephrectomy specimens without any evidence of bN.

Clinical data

Clinical data for the biopsies of the patients and controls were gathered from the files of the referring clinic and included age, sex, systolic and diastolic arterial blood pressure, body height, body weight, body mass index, proteinuria and serum creatinine. These clinical characteristics of the patient and control cohort are given in Table 1. The patients were significantly older than the controls and they had a higher body mass index. This mismatch could not be avoided since almost any kidney from older patients or patients with a higher body mass index that we initially considered as a normal control showed at least minimal bN.

bN and other histologic parameters

A semiquantitative score of bN was applied to all biopsies as recently described [12]. Arteriolar hyalinosis scores (HScores) and fibrosis scores (FScores) were given independently as 0 (absent), 1 (minimal), 2 (moderate) or 3 (severe).

In addition, the area of interstitial fibrosis and cortical tubular atrophy (IFTA) was graded in components as IFTA 0 with <10%, IFTA 1 with <25%, IFTA 2 with <50% and IFTA 3 with ≥50%.

The presence of focal segmental glomerulosclerosis (FSGS) was determined according to the definition by D'Agati *et al.* [13].

Immunostaining

Immunostaining was done for the smooth muscle phenotype markers given in Table 2.

To this end, 3 µm sections from formalin-fixated and paraffin-embedded biopsies were stained for caldesmon, alpha-smooth muscle actin (alpha-SMA), JunB and S100A4 in fully automated Benchmark XT immunostainers (Ventana Medical Systems, Tucson, AZ) with the antigen

Table 1. Clinical characteristics of the patient and the control cohorts

	Patients with bN ($n = 63$)	Controls without bN ($n = 8$)	P
Age (years)*	56 ± 16.4 ($n = 63$)	22 ± 13.4 ($n = 8$)	<0.0001
Sex (female:male)	17:46	2:6	0.90
Systolic blood pressure (mmHg)*	133 ± 26.6 ($n = 56$)	109 ± 14.6 ($n = 8$)	0.0150
Diastolic blood pressure (mmHg)*	77 ± 16.2 ($n = 56$)	66 ± 8.6 ($n = 8$)	0.0349
Body height (cm)	175 ± 10.4 ($n = 49$)	169 ± 28.9 ($n = 7$)	0.7848
Body weight (kg)	83 ± 15.6 ($n = 50$)	69 ± 32.2 ($n = 7$)	0.1889
Body mass index (kg/m^2)*	27 ± 4.8 ($n = 49$)	23 ± 5.5 ($n = 7$)	0.0386
Proteinuria*	25/39 (64%)	0/4 (0%)	0.0248
Serum creatinine (µmol/L)	170 ± 120.1 ($n = 56$)	80 ± 22.5 ($n = 6$)	0.190

*$P < 0.05$.

Table 2. Primary antibodies and antigen retrieval used for the characterization of aVSMCs

Antigen	Vendor, order number	Antigen Retrieval	Concentration
Caldesmon	DakoCytomation, Hamburg, Germany; M3557	pH 6.0	1 + 400
Alpha-SMA	DakoCytomation, Hamburg, Germany; M0851	None	1 + 25
JunB	Acris Antibodies GmbH, Herford, Germany; AP02568PU-N	pH 8.4	1 + 50
S100A4	Abcam plc, Cambridge, UK; ab40722	pH 6.0	1 + 400
Smoothelin	Abcam plc, Cambridge, UK; ab21108	pH 6.0	1 + 100

retrieval methods and primary antibodies listed in Table 2. Bound primary antibody was visualized in brown with the Ultraview Universal DAB Detection Kit (Ventana Medical Systems). Smoothelin staining was done manually after antigen retrieval in citrate buffer pH 6.0 in a pressure cooker. The primary antibody (clone 4A83; Abcam, Cambridge, UK) was incubated overnight at 4°C. Diaminobenzidine (Zytomed Systems, Berlin, Germany) was used as a substrate for a horseradish peroxidase detection system (PolyHRP detection system; Zytomed Systems). Sections were counterstained with haematoxylin. All visible arterioles (defined as less than three cells thickness of the media) were evaluated for each specimen. Immunostaining intensities were graded semiquantitatively as absent, minimal, moderate or strong.

In addition, double immunofluorescence staining was carried out on all nephrectomy specimens from eight patients and eight controls, in which large amounts of tissue could be examined. These stains served to determine whether cells in the arteriolar wall coexpress the secretory marker S100A4 and the contractile markers caldesmon and smoothelin or whether these markers are expressed in a mutually exclusive fashion.

For double immunofluorescence of caldesmon and S100A4, antigen retrieval was performed in citrate buffer at pH 6.0 in a pressure cooker. Primary antibodies were applied in the concentrations stated in Table 2 with 60 min incubation time for caldesmon and S100A4 and with overnight incubation for smoothelin. Cy2- and Cy3-conjugated secondary antibodies (#111-226-003 or #115-165-072; both Dianova, Hamburg, Germany) were applied at a concentration of 1 + 200 with an incubation time of 60 min. Sections were then fixated in formalin for 30 min and stained briefly with Gill's haematoxylin for bright-field microscopy.

Statistical analysis

All statistical analyses were calculated with JMP 8.0.2 (SAS Institute, Cary, NC) on an Apple Macintosh (Apple, Cupertino, CA). For comparison of nominal parameters, chi-square tests were used and for continuous parameters, Wilcoxon tests. Differences were regarded as significant with $P < 0.05$ in two-sided tests. However, in this retrospective exploratory study, P-values can only be regarded as descriptive.

Ethical approval

All studies were carried out according to the Declaration of Helsinki in its latest revision [14] and were approved by the ethics committee of Hannover Medical School.

Results

Clinical parameters in patients and controls

The clinical data of patients with bN and controls without bN are compared in Table 1. Patients with bN were older than controls, had higher systolic and diastolic arterial blood pressures, a higher body mass index and more frequently proteinuria. No difference in body height, body weight or serum creatinine could be found between the cohorts.

Clinical parameters relative to histological parameters

Clinical parameters in relation to histological parameters are given in Tables 3–5.

Table 3. Systolic blood pressure in relation to histological parameters

Parameter	Systolic blood pressure (mmHg)	P
HScore 0 ($n = 11$)	110 ± 18.6	0.0016
HScore 1 ($n = 29$)	125 ± 23.7	
HScore 2 ($n = 14$)	139 ± 25.1	
HScore 3 ($n = 10$)	152 ± 25.9	
FScore 0 ($n = 21$)	114 ± 17.1	0.0023
FScore 1 ($n = 22$)	132 ± 25.3	
FScore 2 ($n = 16$)	139 ± 29.5	
FScore 3 ($n = 5$)	157 ± 21.2	
Only patient cohort		
IFTA 0 ($n = 28$)	122 ± 24.5	0.0037
IFTA 1 ($n = 16$)	136 ± 19.0	
IFTA 2 ($n = 3$)	135 ± 39.1	
IFTA 3 ($n = 9$)	160 ± 23.0	
FSGS present ($n = 7$)	129 ± 25.8	0.0073
FSGS absent ($n = 49$)	130 ± 25.8	

Table 4. Diastolic blood pressure in relation to histological parameters

Parameter	Diastolic blood pressure (mmHg)	P
HScore 0 ($n = 11$)	67 ± 10.1	0.0145
HScore 1 ($n = 29$)	73 ± 14.7	
HScore 2 ($n = 14$)	83 ± 18.2	
HScore 3 ($n = 10$)	84 ± 14.3	
FScore 0 ($n = 21$)	125 ± 23.7	0.0220
FScore 1 ($n = 22$)	77 ± 11.6	
FScore 2 ($n = 16$)	79 ± 22.3	
FScore 3 ($n = 5$)	88 ± 16.8	
Only patient cohort		
IFTA 0 ($n = 28$)	72 ± 15.7	0.0015
IFTA 1 ($n = 16$)	78 ± 15.1	
IFTA 2 ($n = 3$)	70 ± 10.0	
IFTA 3 ($n = 9$)	93 ± 11.3	
FSGS present ($n = 7$)	75 ± 16.2	0.0181
FSGS absent ($n = 49$)	89 ± 10.3	

Systolic blood pressure correlated with HScores ($P = 0.0016$) and FScores ($P = 0.0023$). After exclusion of the control cohort, it correlated with IFTA scores ($P = 0.0037$) and the presence of FSGS ($P = 0.0070$).

Diastolic blood pressures correlated also with HScores ($P = 0.0145$) and FScores ($P = 0.0220$). When analysing only the patient cohort, a correlation was found with IFTA scores ($P = 0.0015$) and the presence of FSGS ($P = 0.0181$).

Patients' serum creatinine correlated with HScores ($P = 0.0013$), FScores ($P = 0.0105$) and with IFTA scores ($P = 0.0010$). No significant correlation was found with the presence of FSGS.

Correlations between glomerular, vascular and tubulointerstitial histological parameters

As shown in Figure 1, the IFTA scores correlated with HScores ($P < 0.0001$) and FScores ($P = 0.0001$).

No significant correlation was found between HScores or FScores and the presence of FSGS.

Markers of aVSMC differentiation

Caldesmon immunostaining was found only in the arteriolar wall in a diffuse cytoplasmic pattern (see Figure 2D–F). The staining intensity in relation to HScores and FScores is given in Figure 3A and B. No significant correlation was found between arteriolar wall immunostaining and HScores (kappa = −0.052235, $P = 0.0558$) and FScores (kappa = −0.03323, $P = 0.0812$).

Alpha-SMA immunostaining was found, similar to that of caldesmon, to be diffusely cytoplasmic (see Figure 2G–I). No significant correlation with HScores (kappa = −0.065, $P = 0.515$) and FScores (kappa = 0.02289, $P = 0.5055$) was found (see Figure 3C and D).

Smoothelin immunostaining was present in a diffuse cytoplasmic pattern (see Figure 2J–L). As shown in Figure 3E and F, staining intensity was significantly decreased with even minimal HScores (kappa = −0.11552, $P < 0.0001$) and FScores (kappa = −0.18724, $P = 0.0033$).

JunB was found in a predominantly nuclear staining pattern in the arteriolar wall (see Figure 2M–O). No significant correlation between arteriolar wall immunostaining and HScores (kappa = 0.195002, $P = 0.4342$) as well as FScores (kappa = 0.473554, $P = 0.7432$) was found (see Figure 3G and H).

S100A4 immunostaining was found in a diffuse cytoplasmic and nuclear pattern in the arteriolar wall (see Figure 2P–R). No significant correlation was found with HScores (kappa = 0.033898, $P = 0.5512$). However, FScores correlated with arteriolar wall immunostaining of FSP-1 (kappa = 0.29318, $P = 0.0321$; see Figure 3I and J).

Arteriolar endothelium was found to be consistently positive for S100A4.

Table 5. Serum creatinine in relation to histological parameters

Parameter	Serum creatinine (μmol/L)	P
HScore 0 ($n = 8$)	88 ± 35.7	0.0013
HScore 1 ($n = 27$)	134 ± 77.9	
HScore 2 ($n = 16$)	153 ± 103.4	
HScore 3 ($n = 11$)	294 ± 159.4	
FScore 0 ($n = 20$)	106 ± 43.2	0.0105
FScore 1 ($n = 20$)	151 ± 95.3	
FScore 2 ($n = 17$)	177 ± 124.5	
FScore 3 ($n = 5$)	370 ± 158	
Only patient cohort		
IFTA 0 ($n = 27$)	117 ± 57.8	0.0010
IFTA 1 ($n = 16$)	148 ± 54.8	
IFTA 2 ($n = 4$)	150 ± 58.2	
IFTA 3 ($n = 9$)	376 ± 152.2	
FSGS present ($n = 7$)	164 ± 115.1	0.5520
FSGS absent ($n = 49$)	212 ± 154.4	

Double immunofluorescence stainings of markers of aVSMC differentiation

Representative examples of normal control arterioles and arterioles with hyalinotic and fibrotic lesions were concordant with the single marker immunoperoxidase staining. The combination of caldesmon and S100A4 showed that aVSMCs were either positive for caldesmon or S100A4. No transitional shift in differentiation with loss of caldesmon and gain of S100A4 could be demonstrated (see Figures 4–6). The same mutually exclusive staining pattern was found in the double stains for smoothelin and S100A4: cells in the arteriolar wall were either completely positive for smoothelin in the normal arterioles (Figure 7) or for S100A4 in the hyalinotic lesions (Figure 8) and in the fibrotic lesions (Figure 9).

Markers of aVSMC differentiation relative to clinical parameters

None of the markers caldesmon, alpha-SMA, smoothelin, JunB or FSP-1 correlated with systolic blood pressure, diastolic blood pressure or serum creatinine (data not shown).

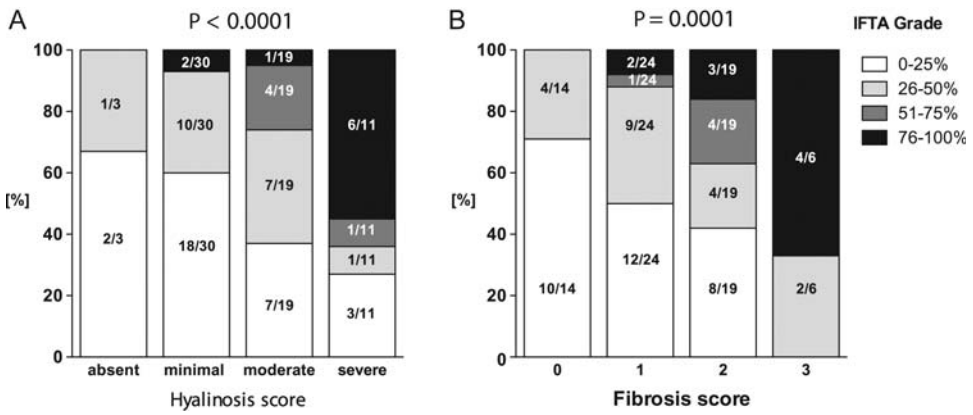

Fig. 1. IFTA scores in relation to HScores and FScores after exclusion of the controls. Both HScore and FScore showed a significant correlation with IFTA scores ($P < 0.05$).

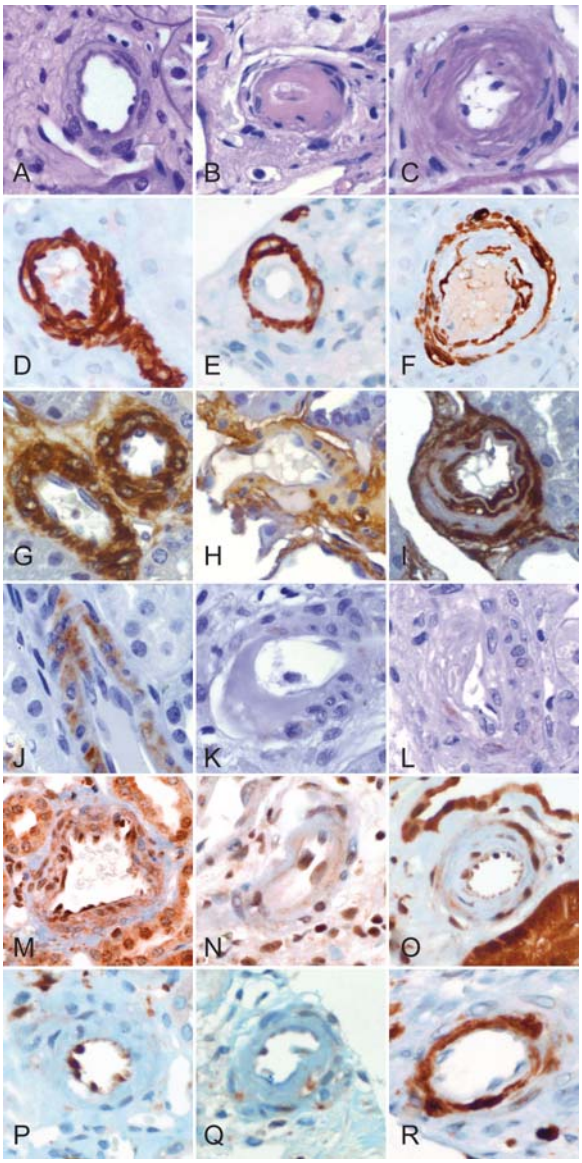

Fig. 2. Histology and immunostains of markers of arteriolar vascular smooth muscle differentiation: (**A**) normal arteriole, (**B**) severe arteriolar hyalinosis, (**C**) severe arteriolar fibrosis. All PAS, original magnification ×600. (**D**) Normal arteriole, (**E**) hyalinotic arteriole and (**F**) fibrotic arteriole with strong caldesmon immunostaining of VSMCs. All immunoperoxidase, original magnification ×600. (**G**) Normal arteriole with strong, (**H**) hyalinotic arteriole with moderate and (**I**) fibrotic arteriole with strong alpha-SMA immunostaining. All immunoperoxidase, original magnification ×600. (**J**) Normal arteriole with moderate, (**K**) hyalinotic arteriole and (**L**) fibrotic arteriole with minimal smoothelin immunostaining. All immunoperoxidase, original magnification ×600. (**M**) Normal arteriole with moderate, (**N**) hyalinotic arteriole with minimal and (**O**) fibrotic arteriole with strong immunostaining for JunB. All immunoperoxidase, original magnification ×600. (**P**) Normal arteriole with absent, (**Q**) hyalinotic arteriole with absent to minimal and (**R**) fibrotic arteriole with moderate S100A4 immunostaining of VSMCs. All immunoperoxidase, original magnification ×600.

Discussion

The present study examines marker proteins of the contractile and the secretory phenotype of VSMCs in bN. Among the classical markers of VSMC differentiation, only the contractile marker smoothelin correlated with arteriolar hyalinosis and fibrosis as expressed by the HScores and FScores in bN. The other examined classical markers of the contractile phenotype caldesmon and alpha-SMA did not. Furthermore, the transcription factor JunB, which regulates the arterial contractile capacity [15] and thus appeared as a potential novel marker of the contractile phenotype, correlated with neither HScores nor FScores. Does this mean that the paradigm of VSMC phenotype is not valid for renal parenchymal aVSMCs in bN? In our opinion, this valuable paradigm should not be abandoned based merely on the results in the special setting of bN. In our opinion, the results just argue for a redefinition and interpretation of the differentiation markers in the context of the type of vessel and disease examined. The notion that caldesmon is a marker of the contractile phenotype stems from examinations in the fetal and adult aorta [16, 17] and from cell culture experiments [18]. The same is true for alpha-SMA [16–19]. Considering the diversity of VSMCs along the course of the vascular tree [20], it appears logical that the markers derived from studies of the aorta do not necessarily apply to renal parenchymal arterioles. Still, smoothelin seems to be a universal marker of VSMC differentiation at all levels of the arterial bed: studies on hypertensive remodelling of the mini-pig aorta have shown a decrease in smoothelin expression [21] quite similar to that in the renal parenchymal arterioles in the present study.

In this study, we also examined the transcription factor JunB in aVSMCs. JunB is a transcription factor that regulates actinomyosin-based cell contraction via the expression of myosin light chain 9 (Myl9). Deletion of JunB has been shown to strongly reduce the contraction capability of arteries *in vivo* [15]. Preserved nuclear JunB immunostaining even in kidneys with higher scores of hyalinosis and fibrosis suggests that JunB-dependent regulation of aVSMC contraction is not disturbed in bN. However, this does not imply that the contraction capacity of arterioles in bN is intact since it also depends on other factors such as arteriolar diameter, cellular and matrix composition of the vessel wall and the local concentration of vasoactive mediators. Neither does the lack of evidence for decreased nuclear JunB immunostaining in VSMCs of hyalinotic or fibrotic arterioles exclude JunB as a marker of the contractile phenotype in VSMCs of other vascular segments and in other disease settings.

While there are many markers of the contractile phenotype of VSMCs, there is currently no widely accepted positive defining marker of the *in vivo* secretory phenotype [22]. Based on *in vitro* data about spindled (contractile) and rhomboid (secretory) VSMCs [23], we speculated that the ‘rhomboid’ marker S100A4, also known as p9Ka, MTS1 or fibroblast-specific protein 1 (FSP1), might serve as a marker of the secretory phenotype in bN. The name FSP1 has been given to S100A4 because of its prominent role in kidney fibrosis [24]. S100A4 was originally thought to be expressed almost exclusively by fibroblasts [24]. Later studies have found S100A4 expression in mononuclear cells, questioning its specificity for fibroblasts [25, 26]. Still S100A4 is a

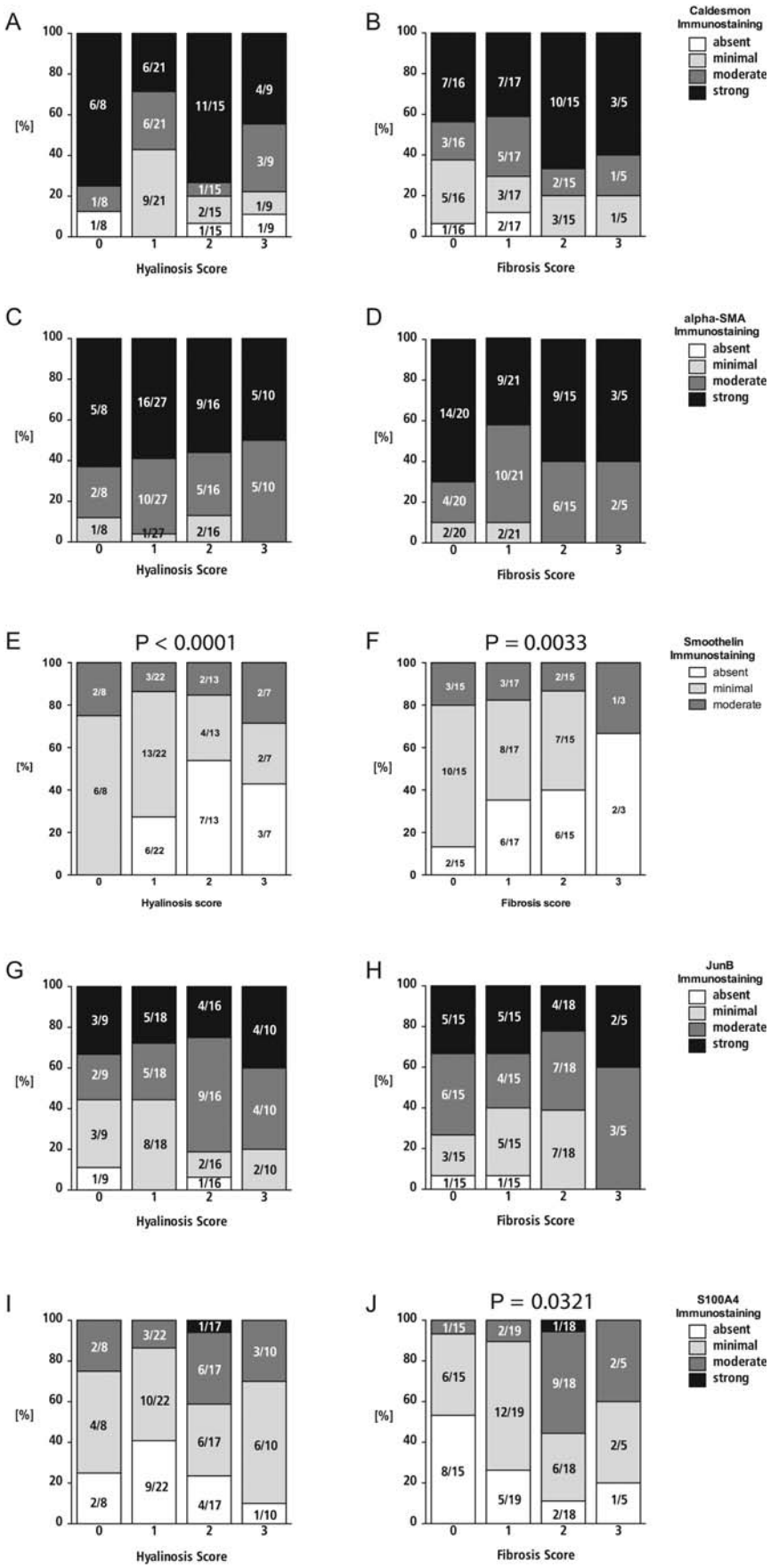

Fig. 3. aVSMC differentiation markers in relation to HScores and FScores. Smoothelin immunostaining of aVSMCs correlated with HScores (kappa = −0.11552; P < 0.0001) and FScores (kappa = −0.18724; P = 0.0033). S100A4 immunostaining correlated with FScores only (kappa = 0.29318; P = 0.0321).

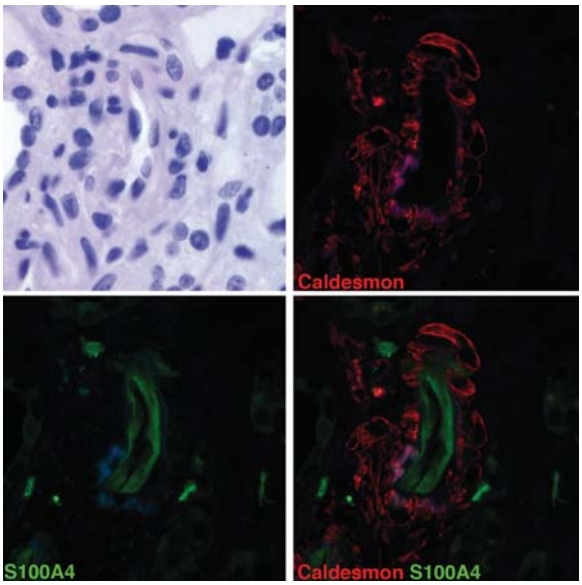

Fig. 4. Distribution of caldesmon (red) and S100A4 (green) in a normal arteriole. The top left panel shows the appearance on the Gill's haematoxylin-stained section with bright-field microscopy for exact morphological reference, while the top right and the bottom left panels show the immunofluorescence staining patterns of caldesmon (red) and S100A4 (green). The bottom right panel shows the merged immunofluorescence staining. Note that all cells in the arteriolar wall are caldesmon positive and S100A4 negative. Only the endothelial lining is positive for S100A4 in this normal arteriole. Combined Gill's haematoxylin stain with caldesmon and S100A4 double immunofluorescence staining on the same section, original magnification ×600.

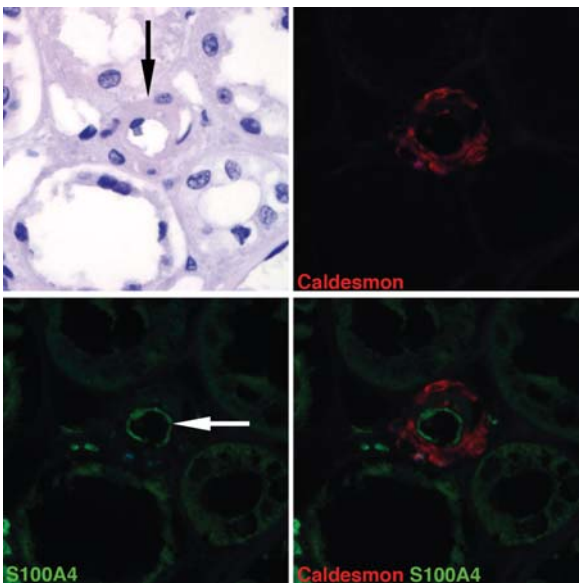

Fig. 5. Double immunofluorescence staining of caldesmon (red) and S100A4 (green) of a hyalinotic arteriole. The top left panel with the Gill's stain shows hyalinosis (black arrow) and the top right and the bottom left panels show the immunofluorescence staining patterns of caldesmon (red) and S100A4 (green). The bottom right panel shows the merged immunofluorescence staining. Note the hyalinosis (black arrow) on the Gill's stain, the S100A4-positive endothelial cells (white arrow) in the bottom left frame and the caldesmon-positive smooth muscle cells in the top right frame. Combined Gill's haematoxylin stain, with caldesmon and S100A4 double immunofluorescence staining on the same section, original magnification ×600.

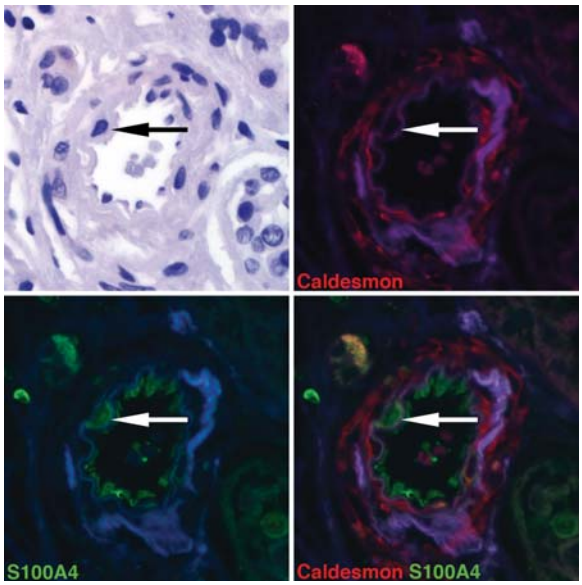

Fig. 6. Double immunofluorescence staining of caldesmon (red) and S100A4 (green) of a fibrotic arteriole. The arteriole with fibrosis is shown in a Gill's haematoxylin stain in the top left frame, the top right and the bottom left frames show the immunofluorescence staining patterns of caldesmon (red) and S100A4 (green). The bottom right panel shows the merged immunofluorescence stain. Note the single S100A4-positive cell (arrow) that is negative for caldesmon. It is situated in the media, just outside of the violet autofluorescent lamina elastica interna. The other smooth muscle cells in the media are caldesmon positive and S100A4 negative. Combined Gill's haematoxylin, caldesmon and S100A4 double immunofluorescence stain on the same section, original magnification ×600.

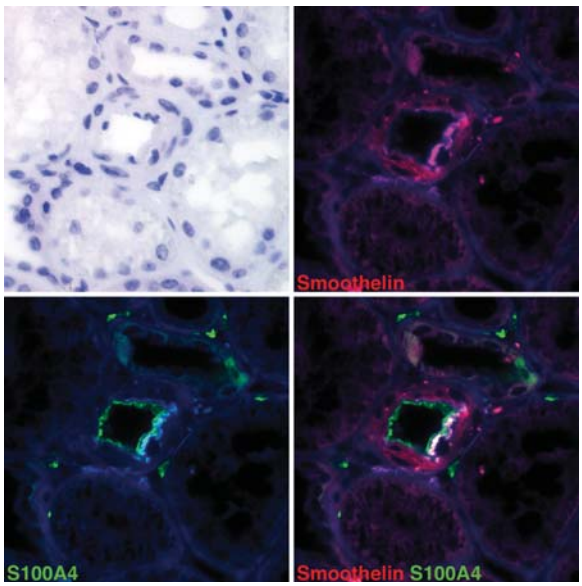

Fig. 7. Distribution of smoothelin (red) and S100A4 (green) in a normal arteriole. The Gill's haematoxylin stain is displayed in the top left frame; the bottom left frame shows the S100A4 immunofluorescence stain in green and the top right frame shows the smoothelin stain in red. The merged frame with smoothelin and S100AB is found at bottom right. Note S100A4-positive endothelial lining and the smoothelin-positive S100A4-negative aVSMCs. Combined Gill's haematoxylin, smoothelin and S100A4 double immunofluorescence stain on the same section, original magnification ×600.

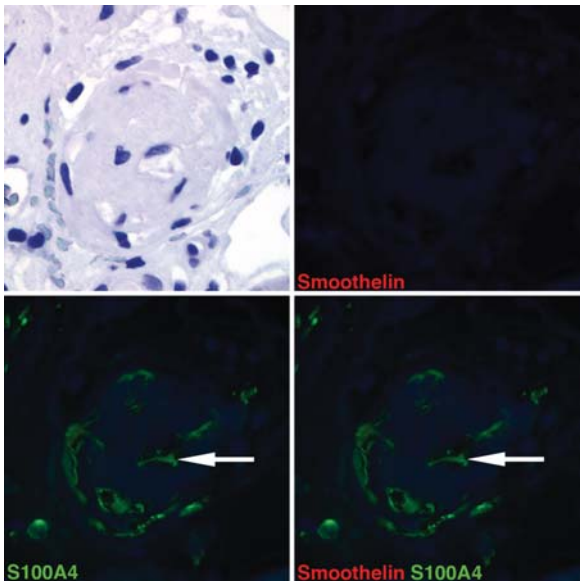

Fig. 8. Distribution of smoothelin (red) and S100A4 (green) in a hyalinotic arteriole. The top left frame shows the Gill's haematoxylin stain, the bottom left frame is the S100A4 immunofluorescence stain in green and the top right frame the smoothelin stain in red. The merged frame with smoothelin and S100AB is shown at bottom right. No smoothelin-positive cells are present in the arteriolar wall. Note the S100A4-positive endothelial cells (arrow). All cells in the hyalinotic media are positive only for S100A4. Combined Gill's haematoxylin, smoothelin and S100A4 double immunofluorescence staining on the same section, original magnification ×600.

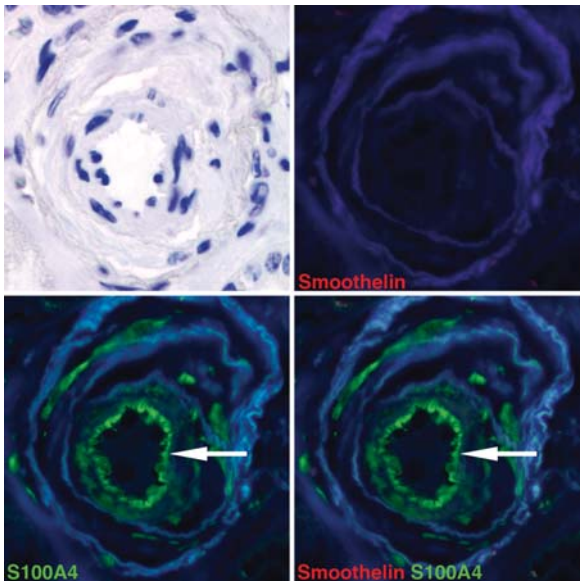

Fig. 9. Distribution of smoothelin (red) and S100A4 (green) in a fibrotic arteriole. The top left frame is the Gill's haematoxylin stain, the bottom left frame displays the S100A4 immunofluorescence stain in green and the top right frame shows the smoothelin stain in red. The merged frame with smoothelin and S100AB is shown at bottom right. No smoothelin-positive cells are present in the arteriolar wall. Note the S100A4-positive endothelial cells (arrow). All cells in the fibrotic wall are positive only for S100A4 and negative for smoothelin. Combined Gill's haematoxylin, smoothelin and S100A4 double immunofluorescence staining on the same section, original magnification ×600.

central protein in the concept of epithelial–mesenchymal transdifferentiation, a process that transforms tubular epithelial cells into fibroblast-like cells, thus contributing to kidney fibrosis. This concept of epithelial–mesenchymal transdifferentiation has recently been seriously challenged [27]. S100A4 is a member of the S100 protein family, all of which share the calcium-binding EF-hand motif [28]. S100A4 forms dimers which bind other proteins, thus allowing cross-bridging for these proteins. A known binding partner of S100A4 is methionine aminopeptidase 2 (MetAP2) [29]. Studies in lung fibrosis have suggested a pharmacologically inhibitable role for MetAP2 in fibroblast and myofibroblast proliferation and collagen deposition [30]. In addition to its intracellular functions, S100A4 is also secreted by VSMCs [31]. The secretion of S100A4 by fibroblasts has been shown to be stimulated by CCL5 [32]. CCL5 in turn is known to be induced by injury in murine arterial VSMCs [33]. *In vitro* data have shown that secreted S100A4 stimulates fibronectin production in fibroblasts [32]. Fibronectin is long known to play an important role in arterial fibrosis (reviewed in [34]). Secreted S100A4 can induce osteopontin in an osteosarcoma cell line [35]. Osteopontin is a major effector of hypertensive arterial fibrosis in rats [36]. Taken together, these literature data and the correlation of S100A4 immunostaining with FScores but not HScores suggest that S100A4 is not only a robust marker of the secretory phenotype in bN but could also have central role in fibrotic remodelling of arteriolar walls in bN.

The double immunofluorescence stainings of caldesmon and smoothelin in combination with S100A4 suggest how the arteriolar walls in bN are remodelled. No coexpression of the contractile markers caldesmon or smoothelin with S100A4 was found. Mutually exclusive expression of the differentiation markers smoothelin and S100A4 is not surprising since both markers probably represent the opposite ends of the aVSMC differentiation. However, the lack of coexpression of S100A4 even with the 'broader' contractile marker caldesmon, as shown in Figure 6, suggests that the transdifferentiation, from contractile to secretory phenotype in the special setting of arterioles affected by bN, is probably not a gradual process but rather an abrupt switch of differentiation. Future research with more combination stainings of selected markers will be necessary to delineate differentiation patterns and pathways in the fibrotic remodelling of arterioles in bN.

In summary, the present study provides the first systematic analysis of classical markers of the contractile and the secretory aVSMC phenotype in bN. The only reliable markers of the contractile phenotype in the setting of bN seem to be the recently established markers ADAMTS13 and smoothelin [12], whereas caldesmon and alpha-SMA immunostaining are stable even in severe hyalinotic and fibrotic arteriolar lesions and thus appear less suitable as a phenotypic marker in bN. In addition, the present results and literature data suggest that S100A4 is not only a robust marker of the secretory phenotype but could also be involved in the pathogenesis of fibrotic lesions in bN. The mechanisms of how S100A4 could orchestrate fibrotic remodelling in bN should be examined in future studies.

Acknowledgements. The authors would like to thank the nephrologists from Bremen, Münster, Offenbach, Wiesbaden and Minden for providing additional clinical data.

Conflict of interest statement. None declared.

References

1. Helmchen U, Wenzel UO In: Tisher CC, Brenner BM *Renal Pathology. With Clinical and Functional Correlations*. Philadelphia, PA: JB Lippincott Company, 1994.
2. Just A Mechanisms of renal blood flow autoregulation: dynamics and contributions. *Am J Physiol Regul Integr Comp Physiol* 2007; 292: R1–R17.
3. Hirota JA, Nguyen TT, Schaafsma D *et al*. Airway smooth muscle in asthma: phenotype plasticity and function. *Pulm Pharmacol Ther* 2009; 22: 370–378.
4. Bara I, Ozier A, Tunon de Lara JM *et al*. Pathophysiology of bronchial smooth muscle remodelling in asthma. *Eur Respir J* 2010; 36: 1174–1184.
5. Hassoun PM, Mouthon L, Barbera JA *et al*. Inflammation, growth factors, and pulmonary vascular remodeling. *J Am Coll Cardiol* 2009; 54 (1 Suppl): S10–S19.
6. Morrell NW, Adnot S, Archer SL *et al*. Cellular and molecular basis of pulmonary arterial hypertension. *J Am Coll Cardiol* 2009; 54 (1 Suppl): S20–S31.
7. Sakao S, Tatsumi K, Voelkel NF Reversible or irreversible remodeling in pulmonary arterial hypertension. *Am J Respir Cell Mol Biol* 2010; 43: 629–634.
8. Rahmani M, Cruz RP, Granville DJ *et al*. Allograft vasculopathy versus atherosclerosis. *Circ Res* 2006; 99: 801–815.
9. Rudijanto A The role of vascular smooth muscle cells on the pathogenesis of atherosclerosis. *Acta Med Indones* 2007; 39: 86–93.
10. Campbell GR, Campbell JH Smooth muscle phenotypic changes in arterial wall homeostasis: implications for the pathogenesis of atherosclerosis. *Exp Mol Pathol* 1985; 42: 139–162.
11. Lindop GB, Boyle JJ, McEwan P *et al*. Vascular structure, smooth muscle cell phenotype and growth in hypertension. *J Hum Hypertens* 1995; 9: 475–478.
12. Bockmeyer CL, Forstmeier V, Modde F *et al*. ADAMTS13—marker of contractile phenotype of arterial smooth muscle cells lost in benign nephrosclerosis. *Nephrol Dial Transplant* 2010; 26: 1871–1881.
13. D'Agati V Pathologic classification of focal segmental glomerulosclerosis. *Semin Nephrol* 2003; 23: 117–134.
14. *World Medical Association General Assembly. Declaration of Helsinki—Ethical Principles for Medical Research Involving Human Subjects*. 2008. http://www.wma.net/en/30publications/10policies/b3/index.html (1 January 2012, date last accessed).
15. Licht AH, Nubel T, Feldner A *et al*. Junb regulates arterial contraction capacity, cellular contractility, and motility via its target Myl9 in mice. *J Clin Invest* 2010; 120: 2307–2318.
16. Frid MG, Shekhonin BV, Koteliansky VE *et al*. Phenotypic changes of human smooth muscle cells during development: late expression of heavy caldesmon and calponin. *Dev Biol* 1992; 153: 185–193.
17. Glukhova MA, Kabakov AE, Frid MG *et al*. Modulation of human aorta smooth muscle cell phenotype: a study of muscle-specific variants of vinculin, caldesmon, and actin expression. *Proc Natl Acad Sci U S A* 1988; 85: 9542–9546.
18. Birukov KG, Frid MG, Rogers JD *et al*. Synthesis and expression of smooth muscle phenotype markers in primary culture of rabbit aortic smooth muscle cells: influence of seeding density and media and relation to cell contractility. *Exp Cell Res* 1993; 204: 46–53.
19. Hungerford JE, Owens GK, Argraves WS *et al*. Development of the aortic vessel wall as defined by vascular smooth muscle and extracellular matrix markers. *Dev Biol* 1996; 178: 375–392.
20. Archer SL Diversity of phenotype and function of vascular smooth muscle cells. *J Lab Clin Med* 1996; 127: 524–529.
21. Hu JJ, Ambrus A, Fossum TW *et al*. Time courses of growth and remodeling of porcine aortic media during hypertension: a quantitative immunohistochemical examination. *J Histochem Cytochem* 2008; 56: 359–370.
22. Rensen SS, Doevendans PA, van Eys GJ Regulation and characteristics of vascular smooth muscle cell phenotypic diversity. *Neth Heart J* 2007; 15: 100–108.
23. Brisset AC, Hao H, Camenzind E *et al*. Intimal smooth muscle cells of porcine and human coronary artery express S100A4, a marker of the rhomboid phenotype in vitro. *Circ Res* 2007; 100: 1055–1062.
24. Strutz F, Okada H, Lo CW *et al*. Identification and characterization of a fibroblast marker: FSP1. *J Cell Biol* 1995; 130: 393–405.
25. Le Hir M, Hegyi I, Cueni-Loffing D *et al*. Characterization of renal interstitial fibroblast-specific protein 1/S100A4-positive cells in healthy and inflamed rodent kidneys. *Histochem Cell Biol* 2005; 123: 335–346.
26. Cabezon T, Celis JE, Skibshoj I *et al*. Expression of S100A4 by a variety of cell types present in the tumor microenvironment of human breast cancer. *Int J Cancer* 2007; 121: 1433–1444.
27. Humphreys BD, Lin SL, Kobayashi A *et al*. Fate tracing reveals the pericyte and not epithelial origin of myofibroblasts in kidney fibrosis. *Am J Pathol* 2010; 176: 85–97.
28. Persechini A, Moncrief ND, Kretsinger RH The EF-hand family of calcium-modulated proteins. *Trends Neurosci* 1989; 12: 462–467.
29. Endo H, Takenaga K, Kanno T *et al*. Methionine aminopeptidase 2 is a new target for the metastasis-associated protein, S100A4. *J Biol Chem* 2002; 277: 26396–26402.
30. Kass D, Bridges RS, Borczuk A *et al*. Methionine aminopeptidase-2 as a selective target of myofibroblasts in pulmonary fibrosis. *Am J Respir Cell Mol Biol* 2007; 37: 193–201.
31. Watanabe Y, Usuda N, Tsugane S *et al*. Calvasculin, an encoded protein from mRNA termed pEL-98, 18A2, 42A, or p9Ka, is secreted by smooth muscle cells in culture and exhibits Ca(2+)-dependent binding to 36-kDa microfibril-associated glycoprotein. *J Biol Chem* 1992; 267: 17136–17140.
32. Forst B, Hansen MT, Klingelhofer J *et al*. Metastasis-inducing S100A4 and RANTES cooperate in promoting tumor progression in mice. *PLoS One* 2010; 5: e10374.
33. Kovacic JC, Gupta R, Lee AC *et al*. Stat3-dependent acute Rantes production in vascular smooth muscle cells modulates inflammation following arterial injury in mice. *J Clin Invest* 2010; 120: 303–314.
34. Intengan HD, Schiffrin EL Vascular remodeling in hypertension: roles of apoptosis, inflammation, and fibrosis. *Hypertension* 2001; 38(3 Pt 2): 581–587.
35. Berge G, Pettersen S, Grotterod I *et al*. Osteopontin—an important downstream effector of S100A4-mediated invasion and metastasis. *Int J Cancer* 2011; 129: 780–790.
36. Giachelli CM, Liaw L, Murry CE *et al*. Osteopontin expression in cardiovascular diseases. *Ann N Y Acad Sci* 1995; 760: 109–126.

Received for publication: 15.9.2011; Accepted in revised form: 30.12.2011